Finite-temperature Casimir force between metal plates: full inclusion of spatial dispersion resolves a long-standing controversy

2006 J. Phys. A: Math. Gen. 39 6741

(http://iopscience.iop.org/0305-4470/39/21/S75)

INSTITUTE OF PHYSICS PUBLISHING JOURNAL OF PHYSICS A: MATHEMATICAL AND GENERAL

J. Phys. A: Math. Gen. **39** (2006) 6741–6752 doi:10.1088/0305-4470/39/21/S75

Finite-temperature Casimir force between metal plates: full inclusion of spatial dispersion resolves a long-standing controversy

Bo E Sernelius

Department of Physics and Measurement Technology, Linköping University, SE-581 83 Linköping, Sweden

E-mail: bos@ifm.liu.se

Received 3 October 2005, in final form 31 October 2005
Published 10 May 2006
Online at stacks.iop.org/JPhysA/39/6741

Abstract

I show that inclusion of spatial dispersion has very small effects on the zero-temperature Casimir force between metal plates, but has dramatic effects at finite temperatures. At high temperatures and/or at large separations, the force is reduced by a factor of 2 compared to the classical perfect-metal result. This is obtained irrespective of if dissipation is included or not. The Nernst heat theorem is not violated even for defectless metal crystals.

PACS numbers: 68.90.+g, 71.10.−w, 71.36.+c, 41.20.−q, 03.50.De, 03.70.+k, 05.40.−a

1. Introduction

The van der Waals [1] and Casimir forces [2–4] may be obtained in terms of the electromagnetic normal modes of the system [5]. These modes are solutions to Maxwell's equations in the specific geometry of the system, in the absence of external sources for the fields. To find the electromagnetic normal modes of a system it is absolutely necessary to take the frequency dependence of the dielectric function into account. In some situations, it is also necessary to include the momentum- or wave-vector dependence, i.e., to take spatial dispersion into account. When this is done, the boundary conditions at the interfaces no longer result in the standard Fresnel equations. This means that the calculations become much more involved. In the calculations of the Casimir force between metal plates, it has uptil now been assumed that spatial dispersion has only minor effects on the result. I will show that this is so at zero temperature, but not at all the cases at finite temperature.

When spatial dispersion is neglected, one may use experimental dielectric data for the materials making up the objects. This is, unfortunately, no longer possible when spatial dispersion is included. Then one has to rely on theoretical model dielectric functions.

There are two quite different predictions in the literature regarding the room-temperature Casimir force for large separations. In one version [6], the result is equal to the perfect-metal result; in the other version [5, 7–10] the result is one half of that result. The result from this work supports the second version.

There is a general consensus in the scientific community as regards the zero-temperature Casimir force, but the community is divided as to how to treat the finite-temperature force. In neglect of spatial dispersion, it all boils down to how the dissipation is treated. In Casimir's original work, the metal plates were treated as ideal metals, i.e., they were treated as totally reflecting mirrors. This produces the first of the two results. For real metals, taking the finite conductivity into account, but neglecting dissipation, one still obtains the first result; in this treatment one uses the simple Drude approximation for the dielectric function; this is the plasma model. Using the Drude approximation, including dissipation, or the experimentally measured dielectric data one obtains the second result. If one includes dissipation and lets the dissipation go towards zero one still obtains the second result. So the force as a function of a dissipation parameter is not continuous at zero dissipation; one may not make an expansion in the dissipation parameter and add a dissipation correction to the ideal metal result. There have been a number of treatments [6] where different prescriptions have been used to force the discontinuity to go away. This line of approach originates in the classical so-called Schwinger prescription [11]. Since all real systems have dissipation any expansion in the dissipation parameter should be made, not from the ideal metal point but from the limit value when dissipation goes to zero.

A particular test of the different approaches has been suggested [6] and applied, namely, if the approach is in agreement with the Nernst heat theorem. The Nernst heat theorem [12] or third law of thermodynamics states that: *The entropy change in a reaction between pure substances approaches zero at* $T = 0$ K. For the van der Waals and Casimir forces between two objects, this translates into the statement that the entropy change, when bringing the objects to infinite separation, approaches zero when the temperature approaches zero. Let us just briefly discuss how the different models handle the Nernst heat theorem in neglect of spatial dispersion. The plasma model obeys the theorem. For real systems with dissipation even when temperature goes to zero the calculations taking dissipation into account obey Nernst's heat theorem [8, 13]. Some of the models involving prescriptions fail. For ideal metal crystals without impurities or other defects, the dissipation parameter vanishes so fast with decreasing temperature that the calculations taking dissipation into account fail to obey the Nernst heat theorem; inelastic scattering processes, such as carrier–phonon or carrier–carrier scattering, vanish at zero temperature due to phase-space limitations; elastic scattering against lattice defects or impurities survives at zero temperature. The fact that the Nernst heat theorem is disobeyed for a perfect metal crystal has been a problem, an academic one, but still a problem. Taking spatial dispersion into account resolves this problem; the Nernst heat theorem is fulfilled even in the absence of dissipation.

In section 2, I give a brief description of how the dispersion forces are related to the electromagnetic normal modes. In section 3, I describe the formalism in the absence of spatial dispersion; I derive the van der Waals and Casimir forces and demonstrate that Nernst's heat theorem is fulfilled for real metals, but not for perfect metal crystals. The same thing is repeated in section 4, but now with spatial dispersion taken into account. Finally, in section 5, I summarize and draw conclusions.

2. Energy and forces at zero and finite temperatures

At zero temperature the dispersion force, F, is obtained from the relation

$$F = -\partial E(d)/\partial d, \tag{1}$$

where E is the internal energy and d is the separation between the objects. The corresponding relation for finite temperatures is

$$F = -\partial H(d)/\partial d, \tag{2}$$

where H is the Helmholtz free energy.

These energies are

$$E = \sum_{\mathbf{k}} \hbar\omega_{\mathbf{k}}(n_{\mathbf{k}} + 1/2), \tag{3}$$

and

$$H = \sum_{\mathbf{k}} \frac{1}{\beta} \ln\left(2\sinh\frac{1}{2}\beta\hbar\omega_{\mathbf{k}}\right), \tag{4}$$

respectively, where the summations run over the electromagnetic normal modes of the system. These modes are characterized by the two-dimensional wave vectors, $\mathbf{k}$, in the plane of the interfaces and $\hbar\omega_{\mathbf{k}}$ is the mode energy. The dispersion curves for the modes are obtained from the solution of Maxwell's equations inside the metal plates and between the plates, and the use of standard boundary conditions at the interfaces; the boundary conditions are that the parallel components of the **E**- and **H**-fields and the normal components of the **D**- and **B**-fields are continuous across the interfaces. This procedure results in conditions of the following type, for having a mode

$$f(\omega, \mathbf{k}) = 0. \tag{5}$$

The solution of this equation gives $\omega(\mathbf{k}) = \omega_{\mathbf{k}}$, which, in general, has several branches.

If the modes are well separated and easy to find one may use equations (3) and (4); if not, one makes use of the so-called generalized argument principle [5], and ends up with the relations

$$E = \hbar\int_0^\infty \frac{\mathrm{d}\omega}{2\pi} \ln f(\mathrm{i}\omega), \tag{6}$$

and

$$H = \frac{1}{\beta}{\sum_{\omega_n}}' \ln f(\mathrm{i}\omega_n), \qquad \omega_n = \frac{2\pi n}{\hbar\beta}, \qquad n = 0, 1, 2, \ldots, \tag{7}$$

respectively. In the last equation $\beta = 1/k_B T$. See [5] for details.

I use, consistently, the idealization that the interface is perfectly sharp; the dielectric function on each side is represented by the bulk function all the way up to the interface. The momentum in the plane of the interfaces is conserved; the momentum perpendicular to the interface plane is not. This means that the boundary conditions are different if spatial dispersion is included or not. The treatment is much simpler when spatial dispersion is neglected. I will treat this case first.

3. Neglecting spatial dispersion

When spatial dispersion is neglected, the dielectric functions have no momentum dependence; they only depend on the frequency. If one may use this approximation the experimentally obtained dielectric functions, for the actual objects one studies, may be used. This is a great advantage. It is also useful to perform calculations with simple model dielectric functions. I will use two of them here.

The first and simplest of the dielectric functions is the simple Drude dielectric function used in the so-called plasma model,

$$\varepsilon(\omega) = 1 - \omega_{\rm pl}^2/\omega^2, \tag{8}$$

which represents a metal when dissipation is neglected. Including dissipation results in the Drude dielectric function

$$\varepsilon(\omega) = 1 - \omega_{\rm pl}^2/[\omega(\omega + {\rm i}\eta)], \tag{9}$$

where the dissipation parameter, η, turns out to have a very important role when spatial dispersion is neglected.

For a system consisting of two half-spaces separated by a gap, there are two types of modes: transverse magnetic (TM) and transverse electric (TE). The conditions for having normal modes in the absence of spatial dispersion can, in the case of half-spaces of the same material, be expressed as [14]

$$[G^{\rm TM,TE}(k,\omega) + 1]^2 - {\rm e}^{-2\gamma^0(k,\omega)d}[G^{\rm TM,TE}(k,\omega) - 1]^2 = 0, \tag{10}$$

where

$$G^{\rm TM}(k,\omega) = \frac{\gamma(k,\omega)}{\gamma^0(k,\omega)}\frac{1}{\varepsilon(\omega)}, \tag{11}$$

and

$$G^{\rm TE}(k,\omega) = \frac{\gamma(k,\omega)}{\gamma^0(k,\omega)}, \tag{12}$$

respectively. The γ functions are

$$\gamma^0(k,\omega) = \sqrt{k^2 - (\omega/c)^2}, \tag{13}$$

and

$$\gamma(k,\omega) = \sqrt{k^2 - \varepsilon(\omega)(\omega/c)^2}, \tag{14}$$

respectively.

Figure 1 shows an example of the dispersion curves for the modes obtained as solutions to equation (10) when the dielectric function in equation (8) is used. In this particular case there are six TM modes and four TE modes. One of the TM modes is a true surface mode; one is for a part of the dispersion curve a true surface mode and for the rest of the dispersion curve of a standing-wave type or waveguide type. The four remaining TM modes and the four TE modes are waveguide modes. The upper solid curve is the boundary of the continuum of bulk-polariton modes. Above this curve the metals can no longer keep the modes in the gap; the modes can propagate freely through the geometry and do not contribute to the dispersion forces. The larger the separation between the plates, the larger the number of modes between the light dispersion curve and the bulk-polariton continuum.

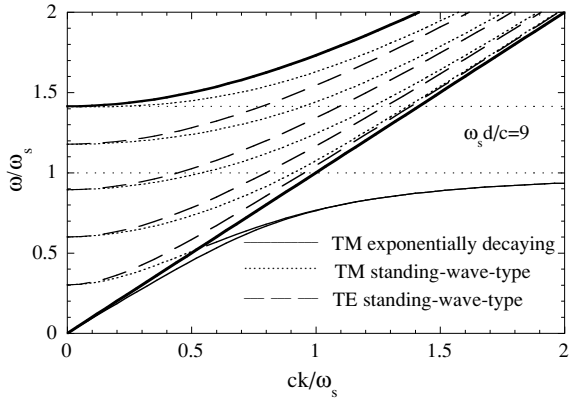

Figure 1. The complete set of normal modes between gold plates (obtained in neglect of spatial dispersion) with a separation of roughly 0.2 μm. The upper thick solid curve is the boundary for bulk-polariton modes and the lower thick solid straight line is the light dispersion curve. The thin solid curves are the modes of true-surface-mode type, the dotted curves are the standing-wave-type TM modes and the dashed curves the standing-wave-type TE modes. Note that one of TM-mode branches changes character when crossing the light dispersion curve.

3.1. The van der Waals and Casimir force

In principle, it is straightforward to calculate the dispersion force from equations (3) and (4) using the modes obtained in the previous section. However, when the separation increases the number of branches grows and/or if one uses the dielectric function in equation (9), or the experimental one, it is not trivial to find the solution to equation (10). If one wants the energies or forces only, it is then much easier to use equations (6) and (7) directly. The results for the energies relative to infinite separation are

$$\Delta E(d) = \hbar \int_0^\infty \frac{\mathrm{d}\omega}{2\pi} \int_0^\infty \mathrm{d}k k \ln\left\{1 - \mathrm{e}^{-2\gamma'^0(k,\omega)d} \frac{[G'^{\mathrm{TM}}(k,\omega) - 1]^2}{[G'^{\mathrm{TM}}(k,\omega) + 1]^2}\right\} + \hbar \int_0^\infty \frac{\mathrm{d}\omega}{2\pi} \int_0^\infty \mathrm{d}k k \ln\left\{1 - \mathrm{e}^{-2\gamma'^0(k,\omega)d} \frac{[G'^{\mathrm{TE}}(k,\omega) - 1]^2}{[G'^{\mathrm{TE}}(k,\omega) + 1]^2}\right\}, \tag{15}$$

for zero temperature and

$$\Delta H(d) = \frac{1}{2\pi\beta} {\sum_{\omega_n}}' \int_0^\infty \mathrm{d}k k \ln\left\{1 - \mathrm{e}^{-2\gamma'^0(k,\omega_n)d} \frac{[G'^{\mathrm{TM}}(k,\omega_n) - 1]^2}{[G'^{\mathrm{TM}}(k,\omega_n) + 1]^2}\right\} + \frac{1}{2\pi\beta} {\sum_{\omega_n}}' \int_0^\infty \mathrm{d}k k \ln\left\{1 - \mathrm{e}^{-2\gamma'^0(k,\omega_n)d} \frac{[G'^{\mathrm{TE}}(k,\omega_n) - 1]^2}{[G'^{\mathrm{TE}}(k,\omega_n) + 1]^2}\right\}, \tag{16}$$

for finite temperature, respectively, where

$$\omega_n = \frac{2\pi n}{\hbar\beta}, \qquad n = 0, 1, 2, \ldots \tag{17}$$

The prime on the summation symbol indicates that the $n = 0$ term is multiplied by the factor $1/2$. The prime on a function indicates that the frequency argument is on the imaginary frequency axis.

The results from these equations using different approximations are shown in figure 2. All results are the interaction energy divided by the zero-temperature (Casimir) result for a perfect metal ($\hbar c\pi^2/720d^3$); all results are for room temperature. The dash-dotted curve is

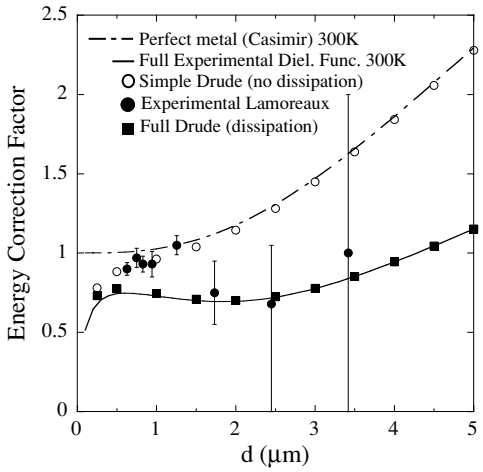

Figure 2. Energy correction factor as a function of separation between two gold plates. All results are for room temperature. The dash-dotted curve is the Casimir perfect-metal result. The solid curve is the result from using the experimental dielectric function and the squares from using the Drude dielectric function [7, 5]; both these results include the effect of dissipation. The open circles are the result from using the simple Drude dielectric function; this does not include dissipation. The solid circles with error bars are the experimental result by Lamoreaux [15].

the result for perfect metals. The result from the simple Drude approximation (open circles) follows the perfect metal result for larger separations. The filled circles with error bars are the experimental result by Lamoreaux [15]. The solid curve is our result [7, 5] where we used the experimental dielectric properties; this means that dissipation was included but no spatial dispersion. Very similar results (squares) are obtained from using the Drude expression, including dissipation, for the dielectric function [5, 7]. Deviations between the solid curve and the squares are expected to occur at small separations where very high frequencies, also, contribute; small separation means that interband transitions and core-level excitations contribute; these are included in the experimental dielectric function, but not in the Drude dielectric function. All curves except the perfect metal curve bend down towards zero when d approaches zero. There is a crossover region, at around 0.05 μm, between the van der Waals region for small separations and the Casimir region for larger separations.

3.2. The Nernst heat theorem

The Nernst heat theorem [12] states that the entropy change in a reaction between pure substances approaches zero as the temperature goes to zero. This would, in the present problem, correspond to the fact that the entropy change, when one brings the two metal half-spaces from a finite separation to infinite separation, should approach zero as the temperature goes towards zero. The entropy, S, is obtained from the Helmholtz free energy, $S = -\partial H/\partial T$.

In figure 3, I show the integrands or summands of equation (16) for the TE and TM contributions, after the momentum integration has been performed. The figure is for gold half-spaces, 1 μm apart. I have chosen to discuss the separation 1 μm since this is the separation where a comparison between the experimental and theoretical temperature dependences of the Casimir effect is most likely to be feasible [7, 15]. Integrands or summands for different separations can be found elsewhere [5]. The temperature dependence comes entirely from the temperature dependence of η [16]. The thin solid curve is for the TM contribution.

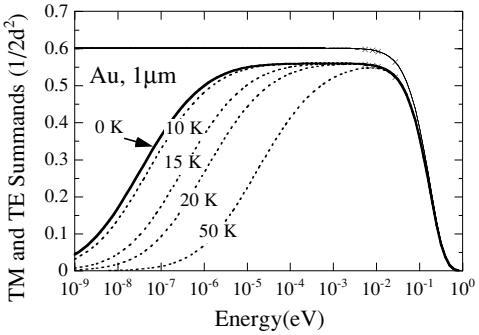

Figure 3. The summands of equation (16) for two gold half-spaces. See the text for more details.

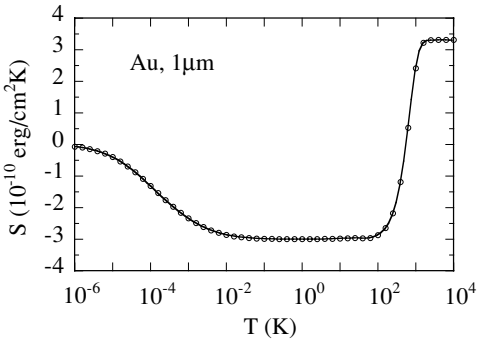

Figure 4. The entropy as a function of temperature for two gold half-spaces. Note that the entropy goes to zero as the temperature approaches zero. Thus Nernst's heat theorem is satisfied.

Here no temperature dependence is visible. The thick solid curve is the TE contribution at zero temperature. The dashed curves are the TE contributions at different temperatures as indicated in the figure. One sees that the temperature dependence occurs for small frequencies, or energies, and extends to higher and higher frequencies with increasing temperature. Each curve carries a cross which indicates the first nonzero frequency value in the summation. The leftmost cross is for 10 K, next is for 15 K and so on. One notes that the cross is always appearing at a frequency where the temperature dependence has vanished. Thus one can neglect the temperature dependence and just use the constant value for η, due to the elastic scattering. In [17] one neglected this very crucial constant and found a violation of the Nernst heat theorem.

I have calculated the entropy (per unit area) in the case of two gold half-spaces and only used the low-temperature constant for η, which equals [18] 3.898×10^{-10} Ω cm. See [8] and [13] for how to obtain results with a limited number of summation points. The results are presented in figure 4. One notes that the entropy change goes to zero as the temperature goes to zero, i.e. the Nernst heat theorem is not violated. One can draw the conclusion that Nernst's heat theorem is fulfilled if the integrands or summands form continuous functions at the low-energy region when the temperature approaches zero. In a real metal with defects, as in figure 3, the TE summand approaches the continuous 0 K curve when the temperature goes to zero. For a defectless metal crystal, the summand would approach a step function with the violation of the Nernst heat theorem as a result. The curve in figure 4 would stay at the lowest

value and would not turn back towards zero when the temperature approaches zero. Thus for metal plates made up from defectless crystals the Nernst heat theorem would be violated in neglect of spatial dispersion.

4. Including spatial dispersion

When spatial dispersion is taken into account the relations resulting from using the boundary conditions become much more involved; the standard Fresnel coefficients no longer result. Furthermore, both the longitudinal and transverse versions of the dielectric function are needed. I use the RPA (random phase approximation) or Lindhard dielectric functions [19]. The functions in [19] are without dissipation. They have been generalized to include dissipation in [20] and [21].

The resulting condition for the modes can be written exactly as in equation (10), but the G-functions are now more complicated. They are [14]

$$G^{\mathrm{TM}}(k,\omega) = \frac{k}{\gamma^0}\tilde{g}_a(k,\omega) - \frac{(\omega/c)^2}{(\gamma^0)^2}\tilde{g}_b(k,\omega) + \frac{k(k-\gamma^0)}{(\gamma^0)^2}\tilde{g}_c(k,\omega) + 1, \qquad (18)$$
$$G^{\mathrm{TE}}(k,\omega) = \tilde{g}_b(k,\omega) + 1,$$

where

$$g_a(k,\omega) = 2k\int_{-\infty}^{\infty}\frac{\mathrm{d}q_z}{2\pi}\frac{1}{q^2\varepsilon_L^{(i)}(q,\omega)}, \qquad (19)$$

$$g_b(k,\omega) = 2\gamma^0(k,\omega)\int_{-\infty}^{\infty}\frac{\mathrm{d}q_z}{2\pi}\frac{1}{\left[q^2-\varepsilon_\perp^{(i)}(q,\omega)(\omega/c)^2\right]}, \qquad (20)$$

$$g_c(k,\omega) = \frac{2(\omega/c)^2k\gamma^0(k,\omega)}{k-\gamma^0(k,\omega)}\int_{-\infty}^{\infty}\frac{\mathrm{d}q_z}{2\pi}\frac{1}{q^2\left[q^2-\varepsilon_\perp^{(i)}(q,\omega)(\omega/c)^2\right]}, \qquad (21)$$

$$g_d(k,\omega) = -2\mathrm{i}\int_{-\infty}^{\infty}\frac{\mathrm{d}q_z}{2\pi}\frac{q_z\,\mathrm{e}^{\mathrm{i}q_z0^+}}{\left[q^2-\varepsilon_\perp^{(i)}(q,\omega)(\omega/c)^2\right]}, \qquad (22)$$

where the three-dimensional wave vector $\mathbf{q}$ is $\mathbf{q} = (\mathbf{k}, q_z)$, where $\mathbf{k}$ is the two-dimensional component parallel to the interface; the tilde above a g-function means the g-function minus the same function except that the dielectric function is put equal to unity. See [14] for details.

4.1. The van der Waals and Casimir force

The forces are obtained from the energies given by expressions identical to equations (15) and (16), but now with the more complicated expressions for the G-functions, given in equation (18). The result is shown in figure 5 as the solid triangles. All other results in the figure are the same as in figure 2. The momentum dependence of the dielectric function cannot be obtained experimentally, so one is forced to use theoretical expressions for the dielectric functions when spatial dispersion is taken into account. In the calculation producing the triangles, I have used the Lindhard [19] dielectric function. For the force calculations, I need the polarizabilities on the imaginary frequency axis. There they are

$$\alpha_L'^0(Q,W) = \frac{y}{2\pi Q^2}\left\{1 + \frac{(W^2+Q^2-Q^4)}{4Q^3}\ln\left[\frac{(Q+Q^2)^2+W^2}{(Q-Q^2)^2+W^2}\right]\right.$$
$$\left. - \frac{W}{Q}\left[\tan^{-1}\left(\frac{Q+Q^2}{W}\right) + \tan^{-1}\left(\frac{Q-Q^2}{W}\right)\right]\right\}, \qquad (23)$$

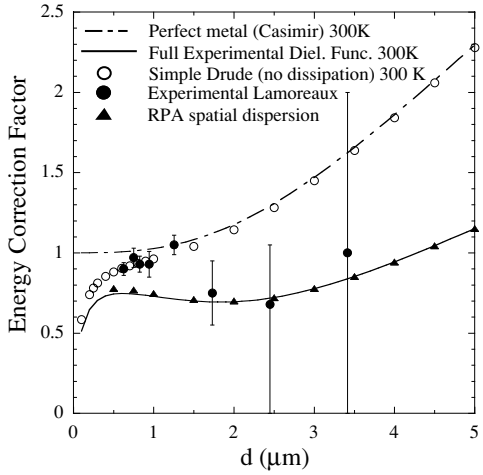

Figure 5. Energy correction factor as a function of separation between two gold plates. All results are for room temperature. The dash-dotted curve is the Casimir perfect-metal result. The solid curve is the result from using the experimental dielectric function; this result includes the effect from dissipation. The open circles are the result from using the simple Drude dielectric function; this does not include dissipation. The solid circles with error bars are the experimental result by Lamoreaux [15]. The triangles are the spatial dispersion result.

and

$$\alpha_{\perp}'^{0}(Q,W)=\frac{1}{8}\frac{y}{\pi Q^2W^2}\left\{-(3W^2-Q^2-Q^4)+\frac{(2WQ^2)^2-(W^2+Q^2-Q^4)^2}{4Q^3}\right.$$
$$\times\ln\left[\frac{(Q+Q^2)^2+W^2}{(Q-Q^2)^2+W^2}\right]+\frac{2W(W^2+Q^2-Q^4)}{Q}$$
$$\left.\times\left[\tan^{-1}\left(\frac{Q+Q^2}{W}\right)+\tan^{-1}\left(\frac{Q-Q^2}{W}\right)\right]\right\}, \tag{24}$$

respectively. The inverse tangent functions are taken from the branch where their absolute values are less than $\pi/2$. I have also performed calculations using the versions [20, 21] of the dielectric functions including dissipation,

$$\alpha_L'(Q,W,\Delta)=\frac{(W+\Delta)\alpha_L'^{0}(Q,W+\Delta)}{W+\Delta\left[\alpha_L'^{0}(Q,W+\Delta)/\alpha_L'^{0}(Q,0)\right]}, \tag{25}$$

and

$$\alpha_{\perp}'(Q,W,\Delta)=\frac{W+\Delta}{W}\alpha_{\perp}'^{0}(Q,W+\Delta), \tag{26}$$

respectively. These calculations led to a very small additional correction. It is very interesting to note that the present result is almost identical to our previous result where the dramatic effect came from dissipation. Compare the present result with the Drude result in figure 2.

In figure 6, I show the integrands in the frequency integrals for the TM- and TE-contributions. I find that the integrand for TE modes becomes very small for small energies, or frequencies, while the TM integrand saturates at a high value. The zero-frequency value for the TE mode is of the order of 10^{-12}. This drop in value has a negligible effect for the zero-temperature result since the drop is for very small frequencies. For the room-temperature result it is of utmost importance. The crosses in the figure show the discrete frequency values

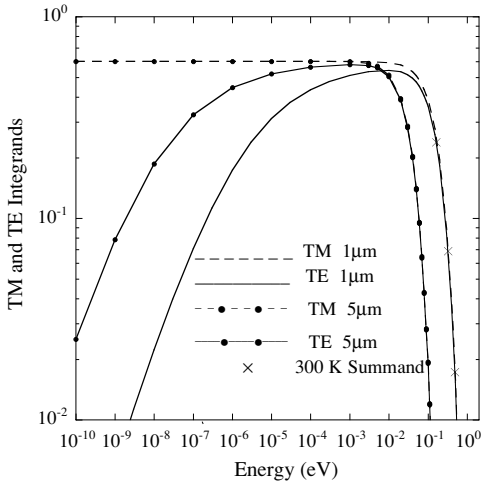

Figure 6. The frequency integrands after the momentum integration have been performed. The integrands for the TM (TE) contribution at 1 μm separation are represented by a dashed (solid) curve. The curves with data points are the corresponding integrands at 5 μm separation. The crosses indicate the points that contribute to the summation at room temperature.

entering the frequency summation. There is also one contribution at zero frequency which I cannot indicate in a log–log figure. The zero-frequency value should be multiplied by a factor $1/2$. One sees that for 1 μm separation, apart from the zero-frequency contribution, only three points have values high enough to be inside the plot. Thus the zero-frequency contribution is very important for the result. For 5 μm separation no point apart from that at zero frequency gives important contribution to the result. Here the zero-frequency contributions completely dominate in the net result. Since the integrand for TE modes has a negligible zero-frequency value only the TM modes contribute to the force at 5 μm separation, at room temperature. At zero temperature both mode types contribute approximately the same to the force at 5 μm separation. The dramatic effects from spatial dispersion are absent at zero temperature. This is in accordance with other recent publications [22, 23]. Those authors did not consider the finite temperature effects.

4.2. The Nernst heat theorem

In figure 6, one sees that even in the absence of dissipation the integrands or summands are continuous functions. This means that Nernst's heat theorem is fulfilled even for a defectless metal crystal.

5. Summary and conclusions

I have demonstrated that, when dissipation is taken into account and spatial dispersion is neglected, the finite-temperature force for real metals at large separations approaches a value which is half the size of the perfect metal result. With this approximation the Nernst heat theorem is fulfilled. For the idealized system of defectless metal crystals the force behaves in the same way but the Nernst heat theorem is violated. Furthermore, I have demonstrated that when spatial dispersion is taken into account the finite-temperature force for metals at large separations approaches a value which is half the size of the perfect metal result; this result is

obtained even in the absence of dissipation. The Nernst heat theorem is fulfilled even in the absence of dissipation. For the idealized system of defectless metal crystals the Nernst heat theorem is fulfilled.

The physical reason for why the spatial dispersion has the effect that the $n = 0$ term is negligible needs to be investigated further. For now, I can only speculate: in the metal there is a continuum of single-particle excitations for finite wave vectors. This continuum comes closer and closer to the frequency axis when the frequency decreases. The continuum actually consists of discrete points. The smaller the separation between the points the bigger the sample. In between these points, there are electromagnetic bulk modes. All these bulk modes contribute in the matching conditions. Since they are inside the continuum the modes are probably very short-lived. This resembles dissipation. All this is automatically taken into account in my calculations along the imaginary frequency axis.

The results taking spatial dispersion into account and the results neglecting spatial dispersion but taking dissipation into account give virtually identical results. This means that in most cases one can, with good confidence, use the experimental dielectric data and neglect spatial dispersion. The important effect that dissipation and spatial dispersion have in common is that the $n = 0$ term in the summation for TE modes has zero or negligible contribution to the results. This means both that the calculations become much simpler to perform and that one may use the actual dielectric data for the plates used in the experiment; the data can vary from sample to sample.

Thus the problem with the Nernst heat theorem is resolved. What still remains to be addressed is the discrepancy between theory and experiment at around 1 μm separation.

Acknowledgments

Financial support was obtained from the Swedish Research Council and the work was partly financed within the EU-project NANOCASE.

References

[1] Langbein D 1974 Theory of van der Waals Attraction *(Springer Tracts in Modern Physics)* (New York: Springer)
[2] Casimir H B G 1949 *J. Chim. Phys.* **47** 407
[3] Casimir H B G and Polder D 1948 *Phys. Rev.* **73** 360
[4] London F 1930 *Z. Phys. Chem.* B **11** 222
London F 1930 *Z. Phys.* **63** 245
[5] Sernelius Bo E 2001 *Surface Modes in Physics* (Berlin: Wiley-VCH)
[6] Geyer B, Klimchitskaya G L and Mostepanenko V M 2003 *Phys. Rev.* A **67** 062102 and references therein
[7] Boström M and Sernelius Bo E 2000 *Phys. Rev. Lett.* **84** 4757
[8] Sernelius Bo E and Boström M 2004 *Quantum Field Theory Under the Influence of External Conditions* ed K A Milton (Princeton: Rinton)
[9] Høye J S, Brevik I, Aarseth J B and Milton K A 2003 *Phys. Rev.* E **67** 056116
Høye J S, Brevik I and Aarseth J B 2001 *Phys. Rev.* E **63** 051101
Brevik I, Aarseth J B and Høye J S 2002 *Phys. Rev.* E **66** 026119
Brevik I, Aarseth J B, Høye J S and Milton K A 2004 *Quantum Field Theory Under the Influence of External Conditions* ed K A Milton (Princeton: Rinton)
[10] Svetovoy V B and Esquivel R 2005 Nonlocal impedances and the Casimir entropy at low temperatures *Phys. Rev.* E **72** 036113
[11] Schwinger J, DeRaad L L Jr and Milton K A 1978 *Ann. Phys., NY* **115** 1
[12] Nernst W 1906 Ueber die Berechnung chemischer Gleichgewichte aus thermischen Messungen *Nachr. Kgl. Ges. Wiss. Gött.* **1** 1–40
[13] Boström M and Sernelius Bo E 2004 *Physica* A **339** 53
[14] Sernelius Bo E 2005 *Phys. Rev.* B **71** 235114

[15] Lamoreaux S K 1997 *Phys. Rev. Lett.* **78** 5
[16] Gray D E 1972 *American Institute of Physics Handbook* (New York: McGraw-Hill)
[17] Bezerra V B, Klimchitskaya G L and Mostepanenko V M 2002 *Phys. Rev.* A **65** 052113
[18] Khoshenevisan M, Pratt W P Jr, Schroeder P A and Steenwyk S D 1979 *Phys. Rev.* B **19** 3873
[19] Lindhard J 1954 *Kgl. Danske Videnskab. Selskab, Mat.-Fys. Medd.* **28** 1
[20] Mermin N D 1970 *Phys. Rev.* B **1** 2362
[21] Kliewer K L and Fuchs R 1969 *Phys. Rev.* **181** 552
[22] Esquivel R, Villarreal C and Mochan W L 2003 *Phys. Rev.* A **68** 052103
[23] Esquivel R and Svetovoy V B 2004 *Phys. Rev.* A **69** 062102